CHAPTER III

RESULTS AND DISCUSSION

Novel oligomeric precursors, namely silatrane complexes, were synthesized via the " OXIDE ONE POT SYNTHESIS " (OOPS) process using inexpensive and widely available SiO_2. This chapter focuses on synthesis, characterization of products, and kinetic studies of SiO_2 dissolution under various reaction conditions.

3.1   Synthesis of Silatrane Complexes

The silatrane complexes were first synthesized directly from SiO_2 and triisopropanolamine in the presence (0.01 mole equivalent) and absence of TETA, under identical conditions. The reaction without TETA took twice as long as the one with TETA. Characterization of the isolated products from both reactions indicated that the structures of the products were almost identical, as discussed in detail below.

3.2   Characterization

3.2.1   Thermogravimetric Analysis

The powder product synthesized from SiO_2 and TIS showed three regions of mass loss in the TGA profile, see Fig.3-1, which was run in air at a heating rate of $10°C/min$.
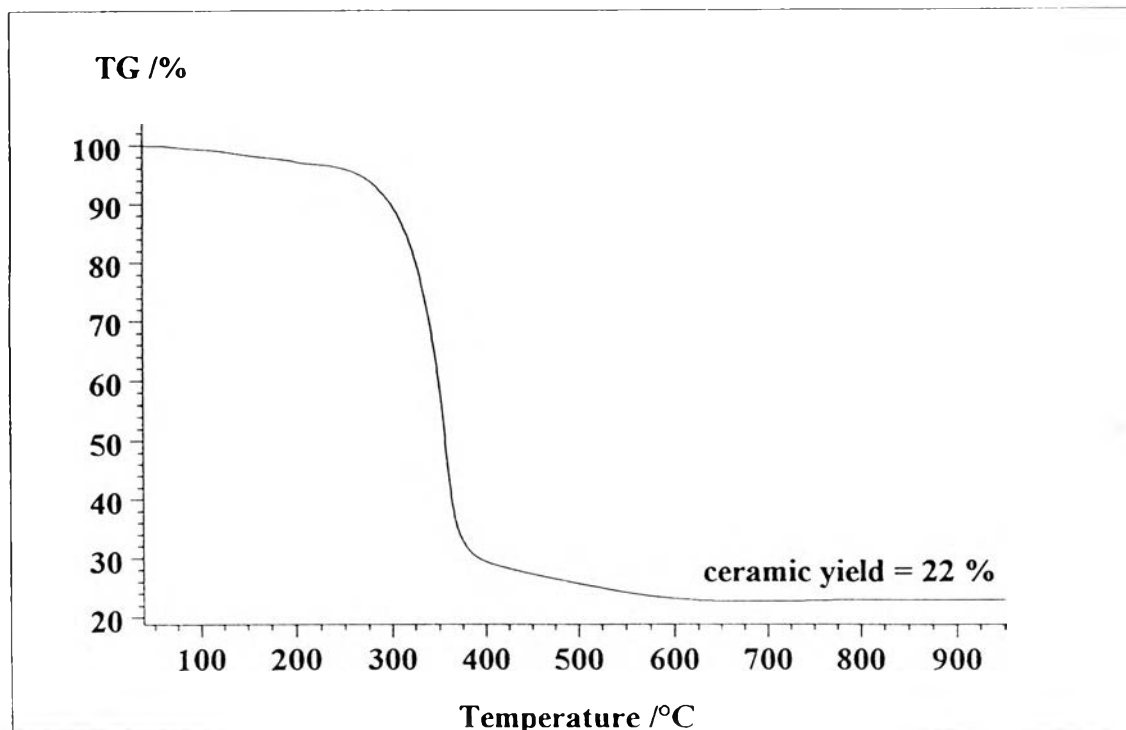
Fig. 3-1   TGA of Precipitated Silatrane Complexes without
TETA.

The first mass loss between 150-250°C corresponds to the loss
of traces of residual EG and TIS. The second mass loss between 290°-370°C
corresponds to organic ligand decomposition, and the final mass loss from
390° to 620°C corresponds to oxidation of residual carbon char. The final
ceramic yield was 22 %, as compared to 21.5 % for the theoretical ceramic
yield based on a final ceramic product SiO_2.

The TGA profile of the dried products from the reaction with
TETA is shown in Fig. 3-2. It showed similar mass losses of products to
those from the reaction without TETA, except the mass loss between 260-
320°C. This region is likely to belong to the excess TETA mixed in the

products and this is supported by NMR data (Table 3-4) which indicate that approximately 15 % TETA is present in the product. As a result, the % final ceramic yield of silatrane with TETA was about 16 %, which is lower than the theoretical ceramic yield, 19.2 %.
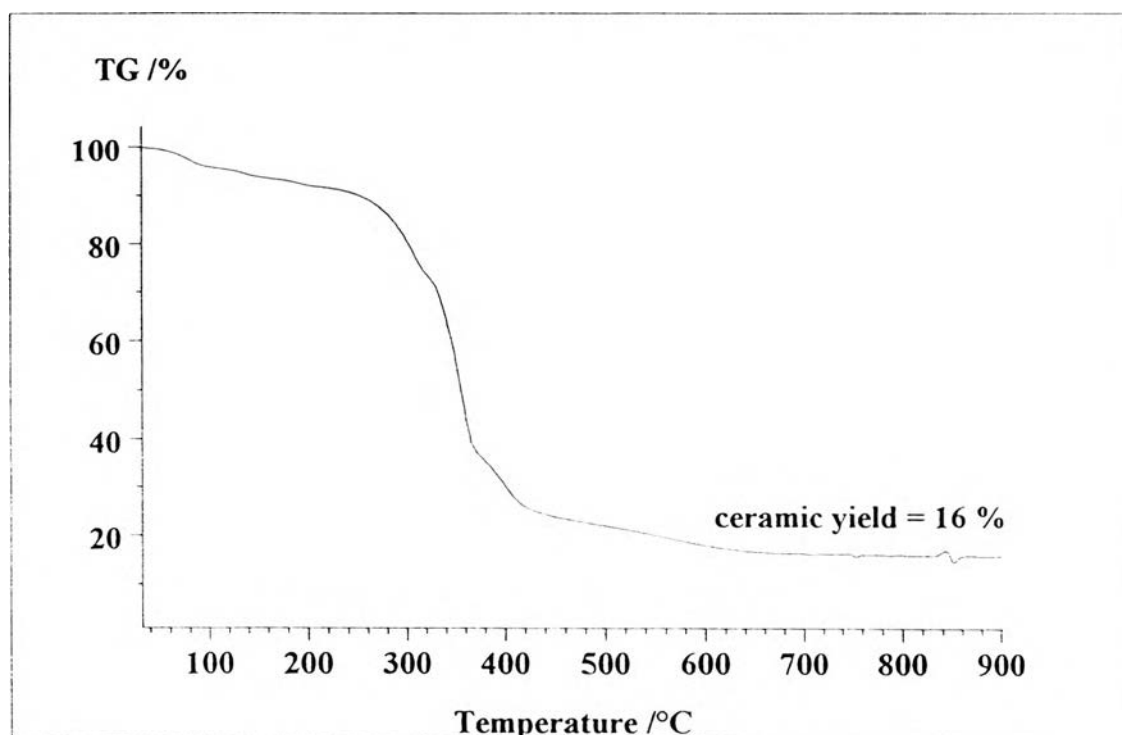

Fig. 3-2   TGA Thermogram of Precipitated Silatrane Complexes
with TETA.

3.2.2 *Differential Scanning Calorimeter*

From DSC data of both products obtained from reaction with and without TETA (Figures 3-3 and 3-4), they could be interpreted similarly to the TGA profiles (Figures 3-1 and 3-2). Both exotherms at about 140°C correspond to decomposition of residual EG, TETA, and TIS. The peaks at 220° and 180°C in Figures 3-3 and 3-4, respectively,

corresponding to the melting point of silatrane complexes, confirm that using catalyst in a reacion always results in shorter oligomers. In the presence of TETA the reaction thus gave products containing shorter unit oligomers, as supported by mass spectroscopy, than the products obtained from the one without TETA. Two exotherms at 280°C and 350°C in Figure 3-3 correspond to the decomposition of organic ligand whereas the endotherm at 410°C is the oxidation of carbon residues.
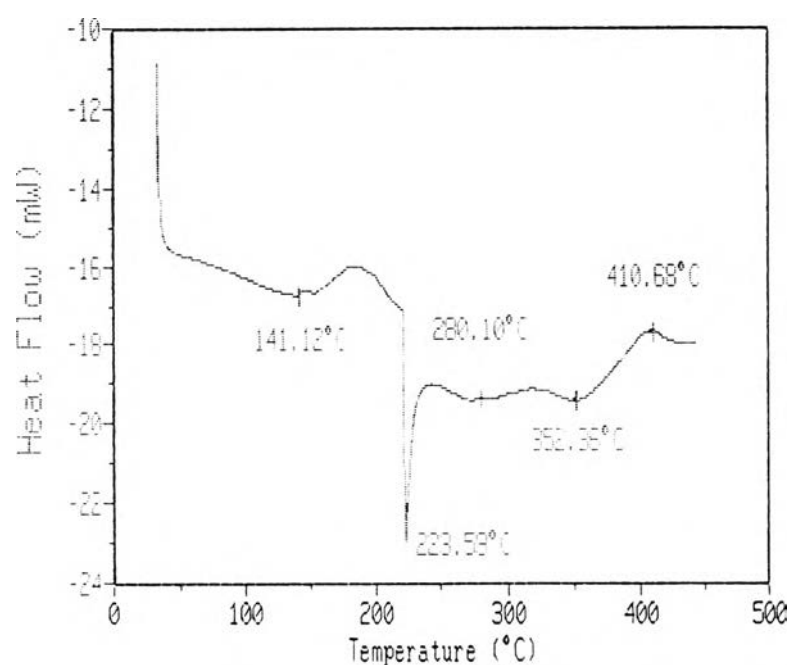

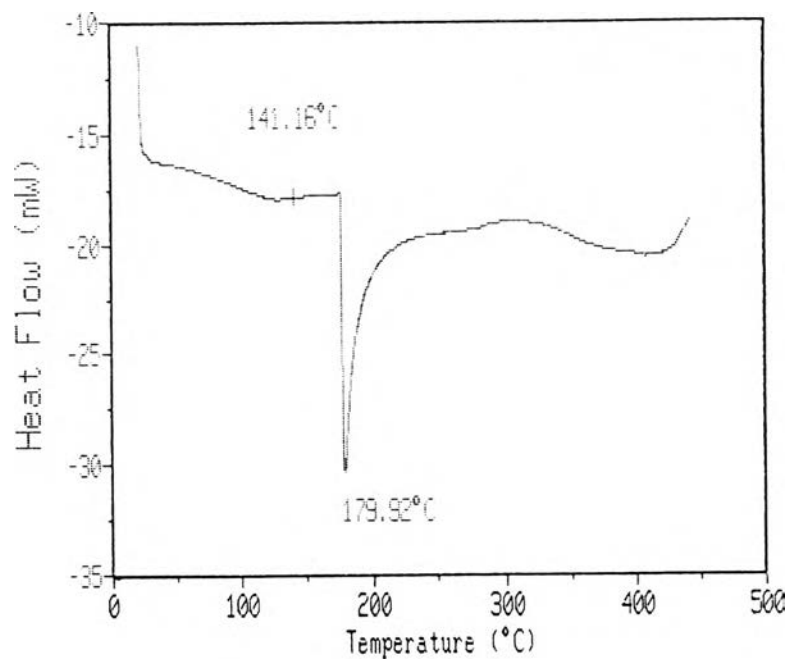**Fig. 3-3**   DSC Thermogram of Silatrane Complexes without TETA

Fig. 3-4   DSC Thermogram of Silatrane Complexes with TETA.

3.2.3   *FAB⁻-MS Spectroscopy*

The FAB⁺-MS spectra fragmentation pattern can be employed to confirm the silatrane complex structures. Tables 3-1 and 3-2 showed the proposed structure of the products, which support the fragmentation patterns in Figures 3-5 and 3-6.
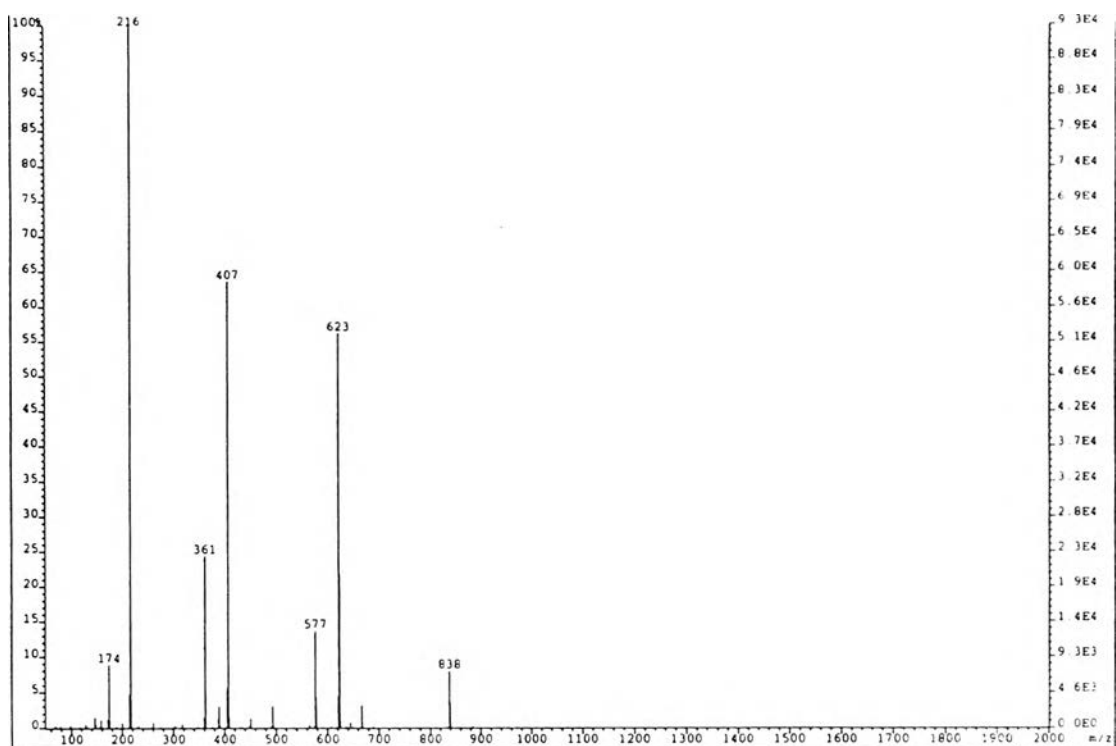
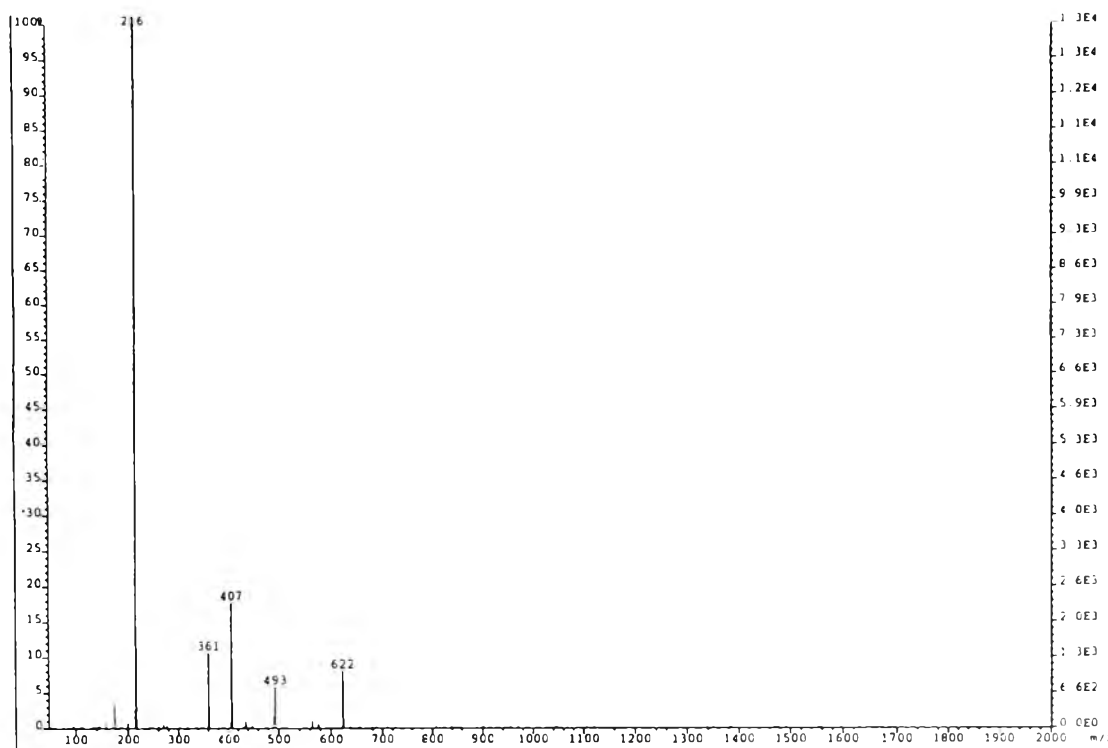**Fig. 3-5**   FAB⁺-MS Fragmentation Pattern of Silatrane Complexes without TETA.

Fig. 3-6   FAB⁺-MS Fragmentation Pattern of Silatrane Complexes
with TETA.

Table 3-1:   The proposed structure and the pattern of fragmentation of the product obtained from the reaction without TETA
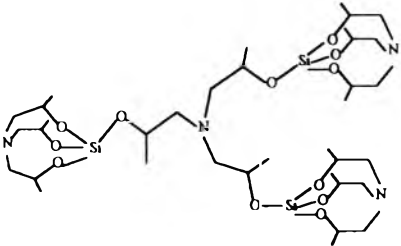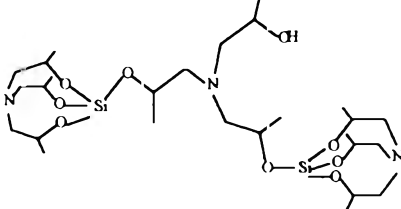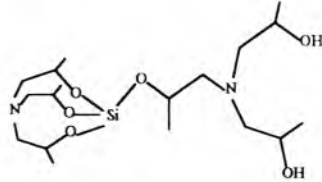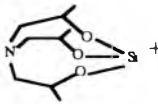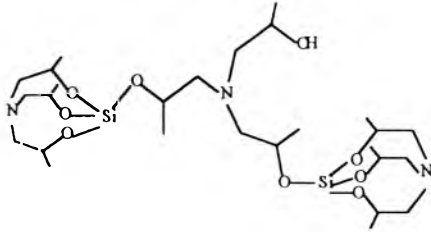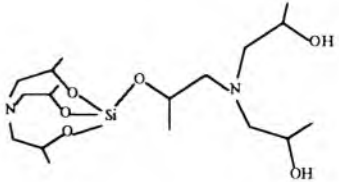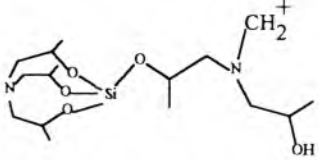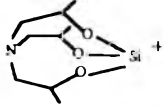
m/e	Intensity	Species
838 (836 + 2H⁺)	8	
623 (621 + 2H⁺)	22	
407 (405 + 2H⁺)	63	
361 (360 + H⁺)	24	
216 (215 + H⁺)	100	

Table 3-2 :   The proposed structure and the pattern of fragmentation of
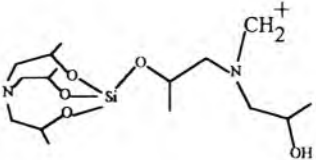
the product obtained from the reaction with TETA

m/e	Intensity	Species
623 (621 + 2H$^+$)	8	
407 (405 + 2H$^+$)	18	
361 (360 + H$^+$)	10	
216 (215 + H$^+$)	100	

The results of FAB$^+$-MS spectroscopy, Fig. 3-5 and Table 3-1 indicate that the product without TETA mainly consists of the oligomer which has the molecular ion peak at m/e 838, and the base peak is the monomer silatrane. The second highest intensity was the fragment with m/e = 407 which has an intensity of 63 %.

The fragmentation pattern of products with TETA was similar to the pattern of the products from the reaction without TETA except that the m/e 838 was absent. This is probably because TETA acted like a accelerator in the reaction which resulted in the shorter chain of oligomers.

3.2.4 Fourier Transform Infrared Spectroscopy

Fig.3-7 and Table 3-3 provide FTIR spectra and data for the precipitated product of the reaction without TETA. They showed the same peaks found in the reaction without TETA which indicated the presence of strong Si-O-C stretching bands at about 1015-1085 cm^{-1}. The peak at 2800-2976 cm^{-1} corresponds to the C-H stretching, whereas the peak at 1380-1460 cm^{-1} results from C-H bending. The peak at 1270 cm^{-1} is assigned to νC-N. The strong peak at 1030-1070 cm^{-1} corresponds to the νC-O and the peak at 560-590 cm^{-1} refers to the Si$\leftarrow$N dative bond.
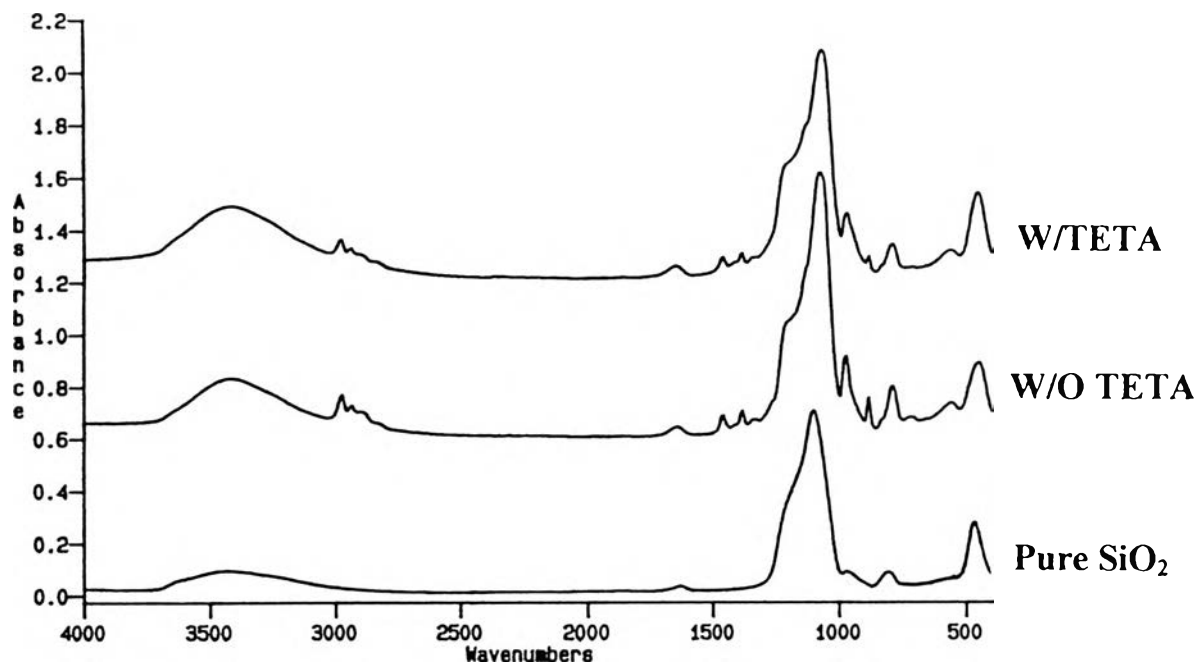
Fig. 3-7 FT-IR Spectra of Silatrane Complexes without and with TETA.

Table 3-3 Assignment of Infrared Spectra of the Products

Characterization	SiO$_2$ (Pure)	SiO$_2$-TIS	SiO$_2$-TIS-TETA
Si ←N stretching[a]	-	560-590 cm^{-1}	560-590 cm^{-1}
Si-O-CH[b]	-	970, 883 cm^{-1}	970, 883 cm^{-1}
C-O[a]	-	1030-1070 cm^{-1}	1030-1070 cm^{-1}
Si-O-CH$_2$[b]	-	1015-1085 cm^{-1}	1015-1085 cm^{-1}
Si-O-Si[b]	1100 cm^{-1}	-	-
C-N[a]	-	1270 cm^{-1}	1270 cm^{-1}
C-H bending[a]	-	1380-1460 cm^{-1}	1380-1460 cm^{-1}
C-H stretching[a]	-	2800-2976 cm^{-1}	2800-2976 cm^{-1}

a : Silverstein et.al, 1991

b :Anderson D. R., 1974

3.2.5 *Nuclear Magnetic Resonance Spectroscopy*

The ^{1}H-, ^{13}C- and ^{29}Si-NMR spectra were used to confirm the structure of the silatrane complexes. ^{1}H-NMR spectrum for the silatrane complexes in d_6-DMSO showed peaks at 0.96-1.12, 2.86-2.91, 3.3, 3.4-3.5, and 4.0 ppm, which are assigned to CH-C$\underline{H}_3$, N-C$\underline{H}_2$, C$\underline{H}_2$-O, CH$_2$O$\underline{H}$ of EG, and C$\underline{H}$-CH$_3$, respectively. The ^{13}C-NMR spectra showed peaks at 20-21, 23, 57.7, 59.2, and 62.5-65 ppm which can be attributed to H$_2$C-CH-$\underline{C}$H$_3$, H$_2$C-CH-CH$_3$, N-$\underline{C}$H$_2$, $\underline{C}$H$_2$-O , $\underline{C}$H$_2$OH of EG, respectively. (Silverstein et.al, 1991;Prakaipetch P., 1995)

^{1}H- and ^{13}C-NMR spectra of the silatrane complexes with TETA showed similar peaks to those obtained from the reaction without TETA, except that ^{1}H-NMR spectra showed peaks at 2.6-2.7, indicating the presence of NH$_2$-C$\underline{H}_2$ in TETA. ^{13}C-NMR showed more peaks at 39-41 ppm also indicating the NH$_2$-$\underline{C}$H$_2$ group of TETA. All the results are presented in Table 3-4. (Silverstein et.al, 1991; Prakaipetch P., 1995)
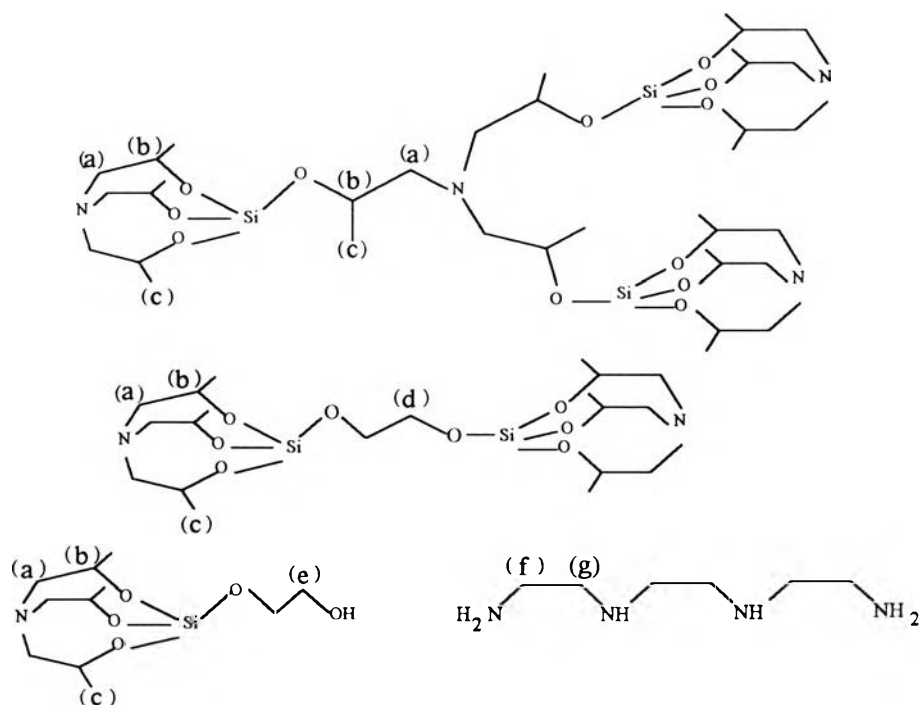
Table 3-4 ^{1}H- and ^{13}C-NMR Chemicalshifts of Silatrane Complexes

(Silverstein et.al. 1991; Prakaipetch P., 1995)

Position	Groups	^{1}H-NMR (ppm)	^{13}C-NMR (ppm)
(a)	N-CH$_2$	2.86-2.91	57.7
(b)	CH-CH$_3$	4.0	23
(c)	CH-CH$_3$	0.96-1.12	20-21
(d)	CH$_2$-O	3.3	59.2
(e)	CH$_2$OH of EG	3.4-3.5	62.5-65
(f)	NH$_2$-CH$_2$ of TETA	2.6-2.7	39-41
(g)	NH-CH$_2$ of TETA	2.9-3.1	60.4-60.7

^{29}Si NMR spectra of the precipitated product of the reactions with and without TETA showed peaks at 96 and 98 ppm respectively, identifying a pentacoordinate Si with dative bond (Sommer L. H.and Bennett O. F., 1959), as shown in Fig. 3-8.

In the above structures, the silicon atom is bonded to 4 oxygen atoms and by a transannular dative bond to the N atom of TIS. Transannular dative bond is not a "normal" silicon-nitrogen bond because the internuclear distances (r_{Si-N}) are considerably longer than an Si-N covalent bond. This was confirmed by the detailed X-ray crystallographic studies by Turley and Boer (1968).
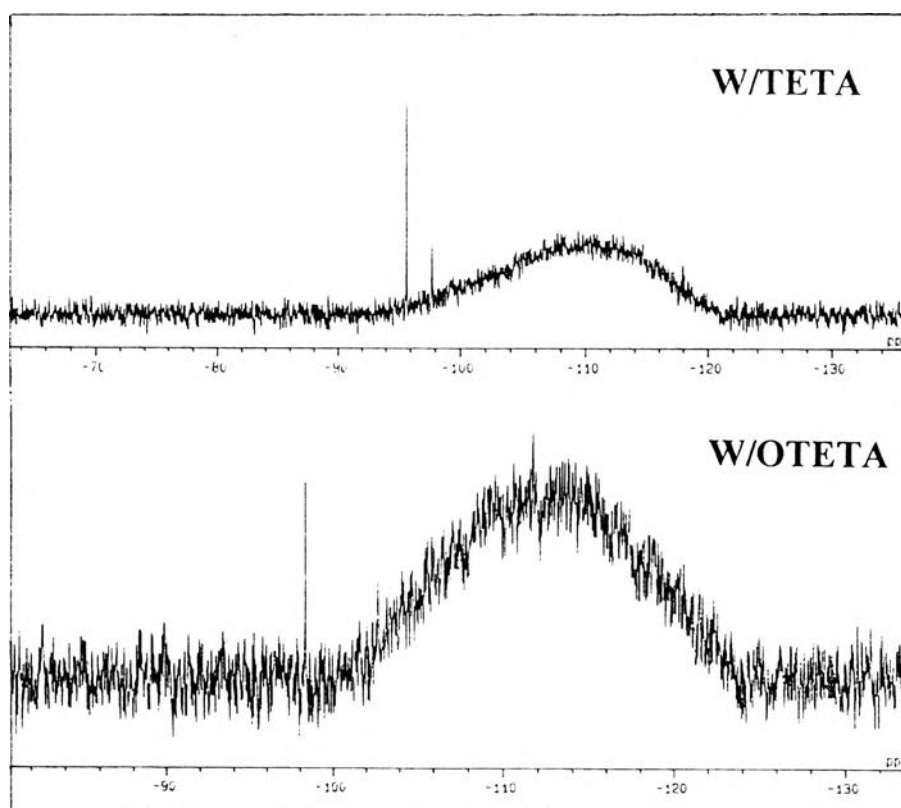

Fig. 3-8 ^{29}Si-NMR Spectra of Silatrane Complexes with and without TETA.

3.3 Kinetic Studies on the Dissolution of SiO_2

These studies were conducted to determine the rate constant, k, reaction order and activation energy of the reaction.

For the determination of the reaction order, by the integral method, the assumption was made that the reaction of SiO_2 with TIS was second order overall and first order with respect to SiO_2 and first order with respect to TIS. The dissolution rate of SiO_2, R, can be expressed as;

$$R = k[SiO_2] [TIS] \qquad (3.1)$$

3.3.1 Dissolution Rate as a Function of the Amount of TIS

TIS concentration was varied from 0 to 120 mmol while fixing SiO_2 at 30 mmol and reaction temperature and time at 200°C and 2 h.., respectively.

The relationship between percentage of dissolved SiO_2 versus TIS concentration showed a linear increase until the amount of TIS approached 60 mmol, as shown in Fig. 3-9 and 3-10. After 60 mmol of TIS, SiO_2 was completely dissolved. The non-zero interception for the reaction run without TIS was a surprising result. This was because SiO_2 dissolves in ethylene glycol, during the process of SiO_2 recovering step, some of the unreacted SiO_2 was lost. That is, the amount of SiO_2 recovered was less than what it should be.
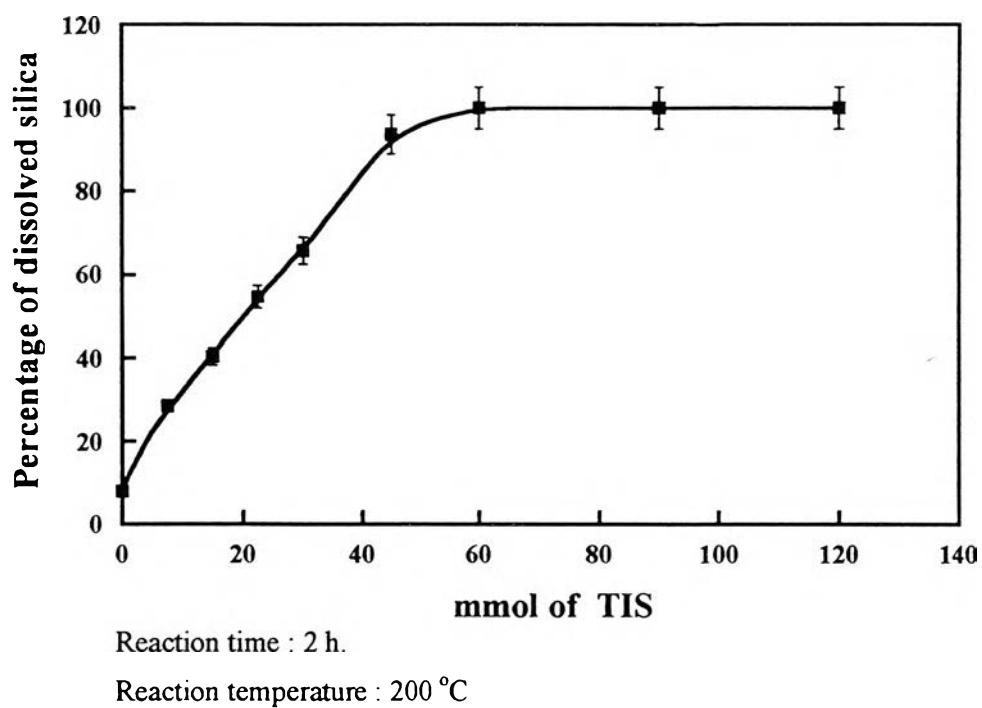
Reaction time : 2 h.

Reaction temperature : 200 °C

Fig. 3-9 The Relationship of % Dissolved Silica for each Variation of TIS.

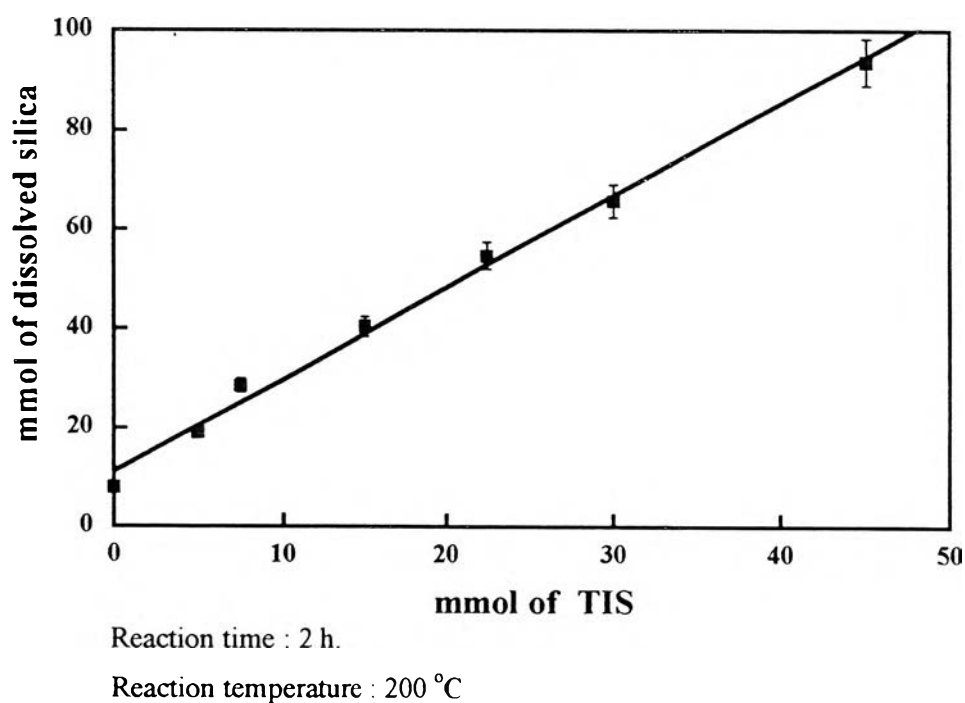Reaction time : 2 h.

Reaction temperature : 200 °C

Fig. 3-10 Effect of TIS Concentration.

3.3.2 Dissolution Rate as a Function of Amount of SiO_2

This study was conducted by fixing the amount of TIS at 30 mmol and varying the amount of SiO_2 from 0 to 60 mmol. The plot of the relationship between the mmol of dissolved and added SiO_2 also showed linear variation, as shown in Fig. 3-11.
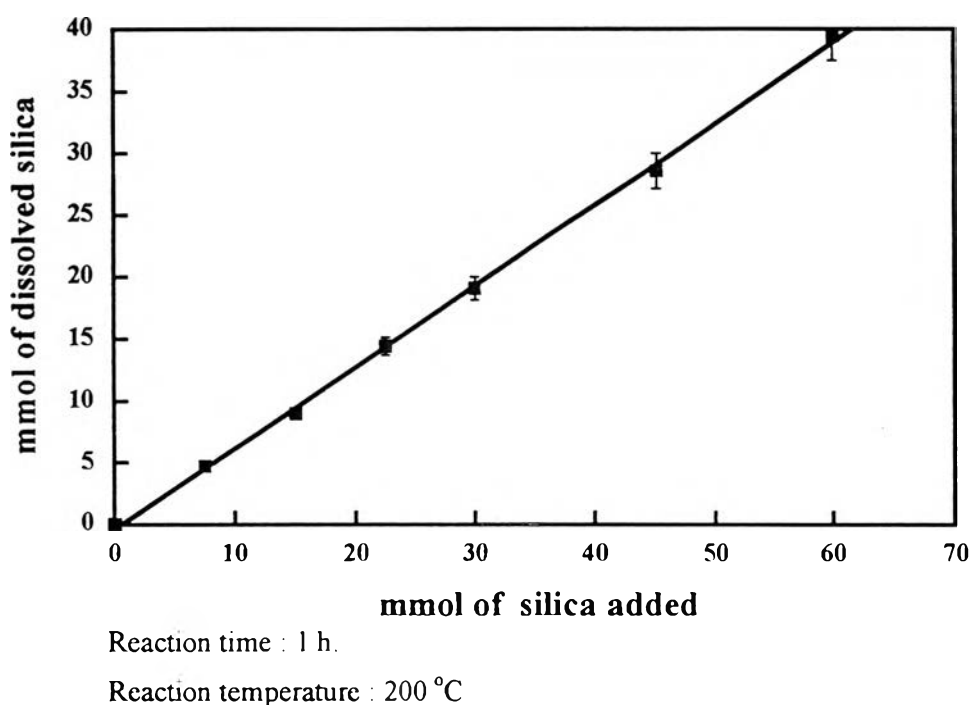

Reaction time : 1 h.

Reaction temperature : 200 °C

Fig. 3-11   Effect of SiO_2 Concentration on the Dissolution of SiO_2.

From both results, we can confirm that the amounts of TIS and SiO_2 have influence on the reaction of TIS and SiO_2. Both plots were linear, therefore the reaction was first order with respect to TIS and first order with respect to SiO_2 which conforms to the dissolution rate expression shown in equation (3.1).

3.3.3 Determination of the Reaction Order

As mentioned previously, the reaction order was determined by the integral method. Therefore, a particular reaction order was first assumed, and the resulting differential equation for the model was then integrated. If the reaction order assumed was correct, then the appropriate plot of concentration versus reaction time corresponding to a particular rate law should be linear.

In this case, the reaction was assumed to be second order overall, first with respect to TIS and first order with respect to SiO_2 Because the experiment was carried out with equal initial concentrations of both reactants, the rate expression and integrated rate law can therefore be obtained from equations (1.10) and (1.11). The plot of reciprocal concentration of the unreacted SiO_2 and reaction time should be linear, with the slope equal to the rate constant.

The reactions were carried out by fixing the amounts of SiO_2 and TIS at 30 mmol. The reaction time was varied from 1 to 75 min at 150°C. The relationship between the reciprocal mmol of unreacted SiO_2 against time was found (Fig. 3-12) to be a straight line, confirming that the assumptions of reaction order of SiO_2 and TIS were correct.
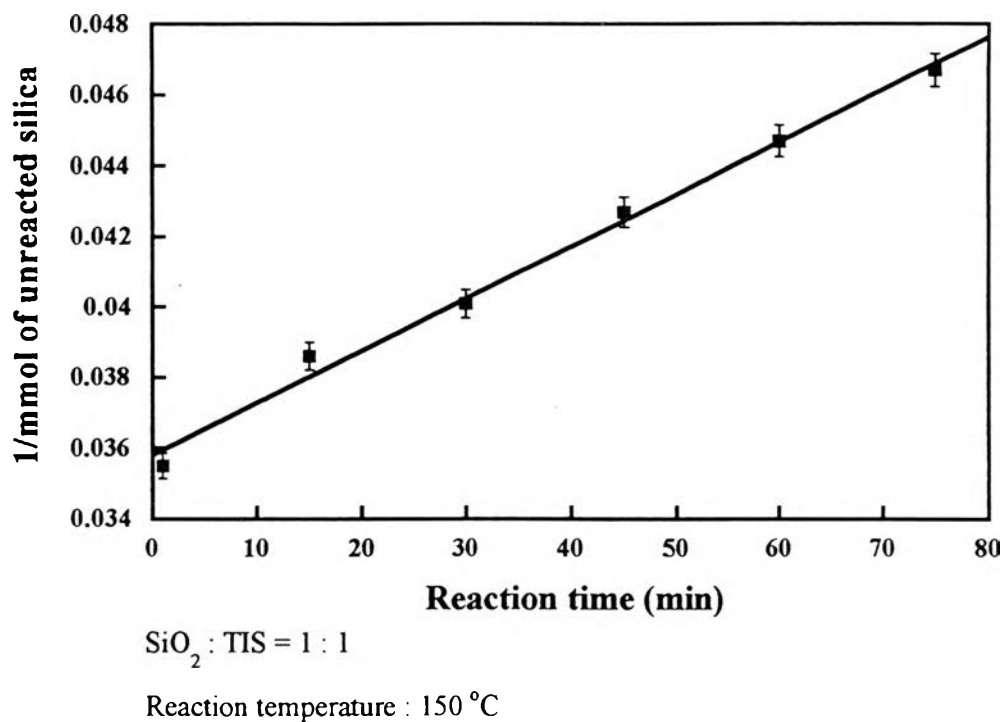
SiO$_2$: TIS = 1 : 1

Reaction temperature : 150 °C

Fig. 3-12   Effect of Reaction time.

3.3.4   *Determination of Reaction Rate Constant and Activation*
        Energy

The reaction rate constant, k, is independent of the concentration of the species involved in the reaction. However, it is strongly dependent on temperature, as expressed in the Arrhenius equation (1.15).

Experiments were conducted by fixing the amounts of SiO$_2$ and TIS at 30 mmol. The reaction temperature was varied from 150°, 170°, to 190 °C. For each reaction temperature, the reaction time was varied from 1 to 75 min. The plots between the reciprocal mmol of unreacted SiO$_2$ vs. reaction time at each temperature gave straight lines with different

rate constants, as shown in Fig. 3-13 and Table 3-5. As expected, reactions run at higher temperature exhibit higher rates of reaction.
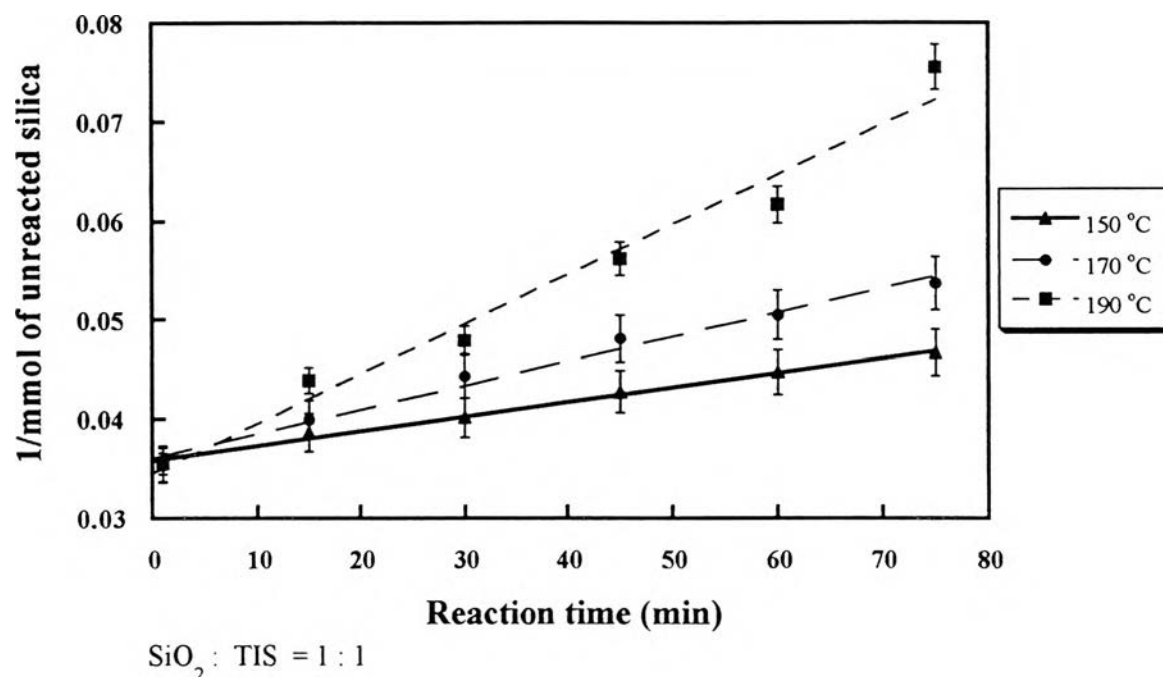

SiO$_2$: TIS = 1 : 1

Fig. 3-13   Effect of Reaction Temperature on the Dissolution of SiO$_2$.

Table 3-5   The Reaction Rate Constants at Various Temperatures

Temp (°C)	1/Temp (1/K)	k (1/mmol.min) × 10^{-4}	ln (k)
150	0.002364	1.3	-8.95
170	0.002257	2.4	-8.32
190	0.002160	5.0	-7.60

Table 3-5 shows the calculated rate constant for each temperature obtained from the slope of the plot which was determined from equation (1.15).

The activation energy could be obtained through the Arrhenius's equation showing to the temperature dependence of specific rate constant, k. After taking the natural logarithm of Arrhenius's equation the following equation was obtained;

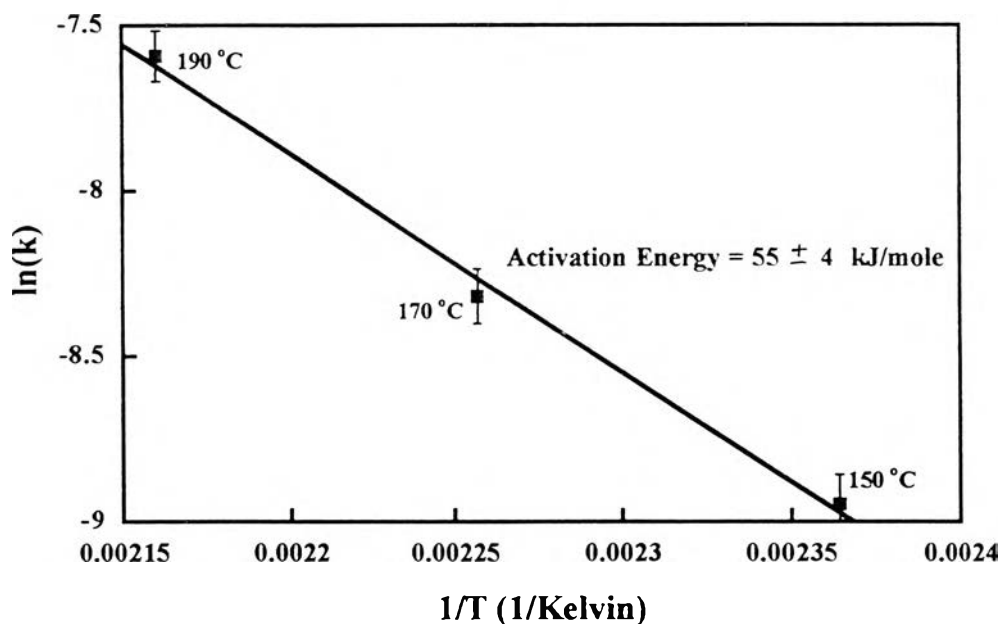$$\ln k = \ln A - \frac{Ea}{R}\left(\frac{1}{T}\right)$$ (3.2)

Fig. 3-14 Determination of the Activation Energy for SiO_2 Dissolution.

The plot of ln(k) and 1/T was in Fig. 3-14, the results was also a straight line with the slope corresponding to the activation energy.

After multiplying the slope with the gas constant (8.314 $Jmol^{-1}k^{-1}$), the activation energy obtained was 55±4 kJ/mol.

3.3.5 *The Dissolution Rate of SiO₂ with TETA as a Function of Time*

The reaction was carried out by fixing the amount of SiO_2, TIS, and TETA at 30 : 30 : 0.3 mmol and varying the reaction time from 1 to 75 min. The reaction temperature was fixed at 170°C. The plot of mmol of reacted SiO_2 versus the reaction time showed faster dissolution of SiO_2 without TETA at the same conditions. The dissolution of SiO_2 with TETA was about 2 times faster, as shown in Fig. 3-15. The reason is that TETA can dissolve SiO_2 which makes it easier and faster to react with TIS.
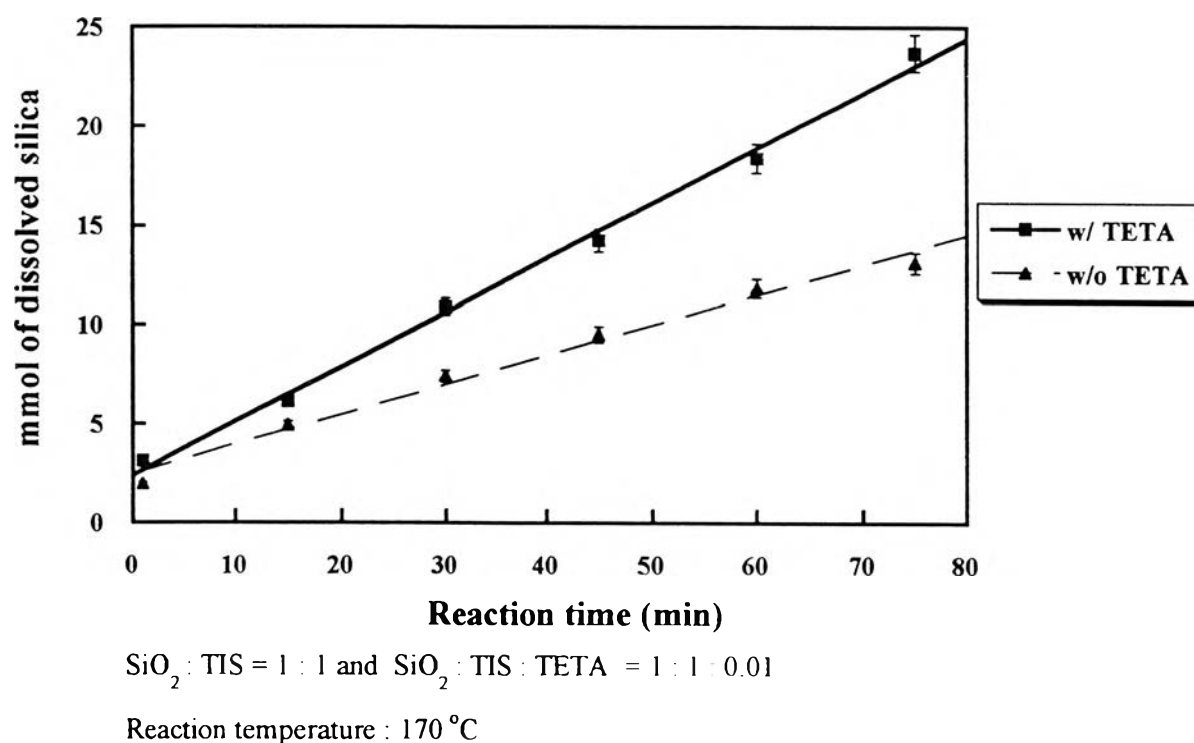

SiO₂ : TIS = 1 : 1 and SiO₂ : TIS : TETA = 1 : 1 : 0.01

Reaction temperature : 170 °C

Fig. 3-15   Effect of TETA on Dissolution of SiO_2.